



Manuscript ID ZUMJ-2012-2055 (R4)

DOI 10.21608/zumj.2021.54107.2055

ORIGINAL ARTICLE

Multi Detector Computed Tomography Application in Diagnosis and Interventional Management of Facial and Neck Swellings in Children

Doaa Ibrahim Hassan¹, Mai Elsayed Mohammed Khamis¹, Ahmed Awad Abd El-Aziz Bessar¹, Ebrika Ali Alsenosi^{2*}

¹ Radiodiagnosis Department, Faculty of Medicine, Zagazig University, Zagazig, Egypt.

² Radiodiagnosis Department, Faculty of Medicine, Omar Elmokhtar University, Libya.

Corresponding author:

Ebrika Ali Alsenosi
Radiodiagnosis Department,
Faculty of Medicine,
Omar Elmokhtar University,
Libya.

Email:

doctorhuda2015@gmail.com

Submit Date 2020-12-18

Revise Date 2021-02-28

Accept Date 2021-05-15

ABSTRACT

Background: Facial and neck swellings are frequently encountered in pediatric medicine, and can present a diagnostic dilemma for the clinicians involved. Neck imaging has always been a diagnostic challenge. Multi-Detector row Computed Tomography is an important imaging modality for characterization and presurgical evaluation of neck masses. The aim of the current study was to evaluate the Multi Detector Computed Tomography (MDCT) in diagnosis and interventional management of facial and neck swellings in children.

Methods: This is a prospective study included 18 patients (7 males and 11 females) their age range from 8 months to up to 16 years, who were referred to radio diagnosis department from clinical departments at Zagazig University hospitals for assessment of facial and neck swellings by ultrasound (US) and computed tomography (CT) during the period from January 2019 to July 2019.

Results: The CT diagnosis of this study was 16.6% Hemangioma, venous malformation and lymphatic malformation same percentage 11.11%, benign soft tissue tumor and facial bone tumor due to thalassemia same percentage 5.55%, congenital swelling 16.6% and infectious facial and neck swellings 22.22%. Sixty percentage of cases after sclerotherapy had complete lesion obliteration and 40 % of them had partial lesion obliteration. Sensitivity of MDCT 87.5%, specificity 100%, PPV 100%, NPV 50% and accuracy 90%.

Conclusions: MDCT imaging is useful for quick and accurate assessment of facial and neck swelling and the possible improvement of any vascular territory in facial and neck swellings by minimal invasive technique of interventional radiology in facial and neck swellings by minimal invasive technique of interventional radiology.

Key words: Hemangioma, vascular malformation, parotid, sclerotherapy



INTRODUCTION

There are several means by which facial and neck masses in children can be subdivided, for example, by age at presentation, anatomical location, including compartments and fascia of the neck, their classical appearance when imaged, or by aetiology [1].

The origins of a facial and neck mass or swelling can vary from congenital causes to acquired conditions such as infection and benign or malignant conditions in soft tissue and/or bone. The clinical history and physical manifestations are the most important factors in the evaluation of

facial and neck swelling and in deciding whether imaging is indicated [2].

When imaging children, the clinicians must be mindful of radiation exposure, and as such, ultrasound (US) is often attempted first. If required, additional acquisition by means of magnetic resonance imaging (MRI) and computed tomography (CT) can be considered [3].

Computed tomography is often the first diagnostic imaging examination performed in patients in whom the presence of a head or neck mass is either evident or suspected. It helps to evaluate the true extent of the disease to best determine surgical and

therapeutic options. This process includes evaluation of the size, location, and extent of tumour infiltration into surrounding vascular and visceral structures [4].

Multi-slice spiral computed tomography (CT) provides volumetric helical data, thereby permitting optimal 3D reconstructions. Rapid scan acquisition reduces motion artifacts as well as permitting phonation studies [5].

Interventional radiology (IR) has evolved rapidly in the past. Imaging technology has advanced over the last two decades. There has also been significant improvement and the development of more sophisticated hardware, with the help of which it is possible to target any vascular territory in the body and carry out therapeutic procedures by minimally invasive technique [6].

The head and neck region is unique in terms of the critical anatomy and vital neurovascular structures involved. It needs detailed knowledge of the head and neck vascular anatomy and special technique to perform vascular IR procedures in the extracranial head and neck [7].

This study aimed to assess the role of MDCT in the evaluation of facial and neck swelling using clinical and interventional management.

METHODS

This study was carried out on 18 patients referred to the Radiodiagnosis Department at Zagazig University Hospitals for assessment of facial and neck swellings by US and CT, during the period from January 2019 to July 2019.

Written informed consent was obtained from all participants, and the study was approved by the research ethics committee of the Faculty of Medicine at Zagazig University. The study was done according to the Code of Ethics of the World Medical Association.

Inclusion Criteria: Patients referred for evaluation of palpable and suspected non-palpable facial and neck masses children (1 month–16 years). Both sex and different masses are diagnosed by ultrasound at the first line.

Exclusion criteria: Patients with contraindications to the contrast study, i.e., serum creatinine >2 mg/dL, or any known or previous history of allergy.

All patients underwent a medical history (onset of facial and neck swellings before or after birth, association with pain or not, fever or not). Clinical examination (focusing on facial and neck swellings, palpable solid or rubbery lumps, tenderness, and redness).

Imaging includes the following:

Ultrasonography: for evaluation and assessment of the mass, it is performed on a Siemens machine with a 7.5–12 MHz superficial probe. Doppler assessment of all cases to assess the presence or absence of vascular flow (central or peripheral). Multi-detector CT for all patients with 128 detectors from Philips Netherlands

Scanning protocol: Patient position: supine, head first, with the neck in the neutral position.

Scanning parameters: tube voltage: 120 kV. Tube current (MAs) reduces tube current in some cases to 80 MAs to reduce the radiation dose. Pitch 1.5:1. The thickness of the slices is 5 mm.

Intravenous (nonionic) iodinated contrast material (1 ml/kg) at rate of 2 ml/sec was administered in 17 patients, excluding one due to bone lesions (ABC). Use general anaesthesia for 13 patients. 2D axial, coronal, and sagittal. 3D volume rendering (VR), maximum intensity projection (MIP)

Image interpretation: images are interpreted and assessed for the location of swelling (face or neck according to anatomical space), size of the lesion, and density (hypo, hyper, or iso dense) by visual assessment. or measurement of the HU (Hounsfield unit) and contrast enhancement (peripheral, central, homogenous, or heterogeneous enhancement).

After a complete investigation and consultation with a physician, we divided the 18 cases into 2 groups: vascular and non-vascular lesions. In five cases, MRI confirms the diagnosis of a vascular lesion: two lymphatic malformations, two venous malformations, and a hemangioma, which is then treated with sclerotherapy: Group (1): Sclerotherapy in 5 cases confirms the diagnosis by MRI, Group (2): Surgical confirmation of diagnosis by surgery and histopathology in 7 cases, and Group (3): Medical treatment confirms and follows up on the diagnosis in six cases. Non-vascular lesion subdivided into surgical group 7 cases (thyroglossal cyst, brachial cleft cyst, lipoma, ranula, left thyroid nodule, submental abscess, and fibrous dysplasia), and medical group 6 cases (two cases of infantile hemangioma, thalassemia, periorbital cellulitis, infected lymph nodes, and parotitis) confirm the diagnosis by treatment and follow-up. Position: head-first supine.

Position the head in the head and neck coil and centre the laser beam localizer over the nose tip. General anaesthesia was administered to all patients except one (age 15 years).

Sclerotherapy is performed on patients with vascular lesions using a tiny instrument such as a 22- or 24-gauge needle percutaneous route, a 10-ml syringe, and general anaesthesia under fluoroscopy X-ray.

Patient preparation: Before procedures, complete investigations such as the CBC (complete blood count), RFT (renal function test), LFT (liver function test), PT (prothrombin time), PTT (partial thromboplastin time), INR (international normalised ratio), and checkups on pulse rate, blood pressure, respiratory rate, and hydration level.

Technique :

Under fluoroscopy, the lesion was identified using ultrasound or clinical examination, and the contents were aspirated and injected with non-ionic contrast under a fluorescence screen. For venous malformations, absolute alcohol was used as the main sclerosant agent, while for lymphatic malformations, bleomycin was the sclerosant agent. The sclerosant agent is then injected to ensure the lesion's extension and dimensions. The procedure was repeated after a few minutes to ensure the state of the lesion and the area that had been obliterated. The dose of alcohol did not exceed 0.5 mg/kg, and the dose of bleomycin was about 0.25 units/kg.

After-care included antibiotics, corticosteroids, and anti-inflammatory medications.

Follow up: Ultrasound for every case before and after procedures of *CT and/or MRI scan*.

Case (1): (A) Ultrasound shows a well-circumscribed cystic lesion in the supraclavicular region measuring about 2x6 cm with no calcification or colour flow, (B) On CT with contrast, a cystic lesion is seen in the left posterior triangle with no extension to the thoracic inlet. (C) MRI: T1 and T2 coronary MR images show an isointense cystic lesion in the left posterior thigh. (D) Sclerotherapy: fluoroscopic image of an interventional procedure for percutaneous needle injection of bleomycin in lymphatic malformations in the LT posterior triangle of the neck while under general anesthesia. After Sclerotherapy: (I) Ultrasound: show complete obliteration of lymphatic malformations in the left posterior triangle and supraclavicular region in ultrasound; (F): axial CT with contrast after complete sclerotherapy treatment and complete obliteration (Fig. S1 and S2).

STATISTICAL ANALYSIS

Data collected throughout history (basic clinical examination, laboratory investigations, and outcome measures) was coded, entered, and analysed using Microsoft Excel software. The data was then imported and analysed using the Statistical Package for the Social Sciences (SPSS) version 20.0 software. The following tests were used to test for significance of differences based on

the type of data (qualitatively represented as number and percentage, and quantitatively represented by mean SD): difference and association of qualitative variables by the Chi-square test (X^2). Differences between quantitatively independent groups by t test or Mann Whitney, paired by a sign test. **For categorical data, the chi-square test² was used to test the association variables.**

RESULTS

In 38.8% of cases, vascular lesions were discovered. 16.66% of them had hemangiomas, 11.11% had venous malformations, and 11.11% had lymphatic malformations. Non-vascular lesions were found in 61.1% of patients; 22.22% of them had infection; 16.66% had congenital disease; 5.55% of them had a benign soft tissue tumour; 5.55% had a facial bone deformity (thalassemias; 22.22% of them had infection; 16.66% had congenital disease; 5.55% of them had a benign soft tissue tumor; 5.55% had a facial bone deformity (thalassemia); and 5.55% had fibrous dysplasia (Table 1). The ultrasound characteristics of benign soft tissue tumours were well-defined in 11% of cases, iso- to hyperechogenicity in 5.5%, and peripheral low flow in 5.5% (Table 2). CT features of benign soft tissue swellings include 11% well-defined edges and hypodensities, contrast enhancement, and calcification (5.5%; Table 3). Only one case of fibrous dysplasia in ultrasound showed a well-defined hypoechoic lesion, and one case of facial thalassemia in ultrasound showed an ill-defined hypoechoic lesion with lymphadenopathy (Table 4). The fibrous dysplasia in CT is hyperdense with no contrast enhancement, and the facial thalassemia in CT is an ill-defined, hypodense mass swelling with mandibular ramus destruction and no contrast enhancement (Table 5). In 33.3% of cases, medical treatment was used, in 38.9% of cases, surgical treatment was used, and in 27.8% of cases, sclerotherapy was used (Table 6). The MDCT diagnosis was confirmed in 33.3% of cases by medical treatment, 33.3% by surgery, and 22.2% by MRI (Table 7). In 2 cases, the diagnosis was accurate (1 case confirmed by surgery and histopathology, 1 case confirmed by MRI) (Table S1). The sensitivity of MDCT was 87.5%, specificity 100%, PPV 100%, NPV 50%, and accuracy 90% (Table S2). The study showed that 60% of cases undergoing sclerotherapy had complete lesion obliteration, and 40% of them had partial lesion obliteration (Table S3).

Table 1 Distribution of the studied patients:

	Mean ± SD	Median (range)
Age (years)	3.18 ± 3.72	1.4 (61 days – 14 years)
	N=40	%
Diagnosis:		
Cardiac	8	20
Respiratory	8	20
Neurological	20	50
GIT	3	7.5
Multiorgan failure	1	2.5
Mechanical ventilation:		
Yes	22	55
No	18	45
Outcome		
Survivors	37	92.5
Dead	3	7.5

Table 2 Comparison between RDW in the studied patients and patient's outcomes:

RDW %	Results		Test	
	Studied patients	Outcomes	t	p
	Mean ± SD	Mean ± SD		
First day	20.93 ± 2.76	15.9 ± 3.23	2.616	0.013*
Fourth day	18.23 ± 5.51	16.21 ± 3.39	0.954	0.346
Seventh day	16.13 ± 0.75	16.65 ± 3.33	-0.263	0.794
p (F)	0.418	0.196		

*, p<0.05 is statistically significant; t, Independent sample t test; F, repeated measure ANOVA

Table 3 Correlation between RDW at each day and hematological indices on the same day among the studied patients:

	RDW first day		RDW fourth day		RDW seventh day	
	r	p	r	p	r	p
WBCs ×10 ³ /mm ³	0.229	0.156	0.09	0.581	0.426	0.006*
RBCs million/mm ³	0.243	0.13	0.125	0.443	-0.019	0.91
Hemoglobin g/dl	-0.14	0.388	-0.101	0.535	-0.43	0.006*
PCV (%)	0.051	0.755	-0.195	0.228	-0.29	0.069
MCV (fl)	-0.566	<0.001**	-0.599	<0.001**	-0.441	0.004*
MCH (pg)	-0.324	0.041*	-0.341	0.031*	-0.356	0.024*
MCHC (g/dl)	-0.434	0.005*	0.088	0.587	-0.298	0.061
Platelet count ×10 ³ /ml	-0.198	0.22	-0.186	0.249	-0.252	0.117

*, p<0.05 is statistically significant; **, p≤0.001 is statistically highly significant; WBCs, white blood cells count; RBCs, red blood cells count; PCV, packed cell volume; MCV, mean corpuscular volume; MCH, mean corpuscular hemoglobin; MCHC, mean corpuscular hemoglobin concentration

Table 4 Correlation between RDW values over different days among the studied patients:

RDW %	RDW first day		RDW fourth day		RDW seventh day	
	r	p	r	p	r	p
1 st day	1		0.697	<0.001**	0.64	<0.001**
4 th day	0.697	<0.001**	1		0.672	<0.001**
7 th day	0.64	<0.001**	0.672	<0.001**	1	

*, p<0.05 is statistically significant; **, p≤0.001 is statistically highly significant

Table 5 Correlation between RDW and CRP, kidney function tests, liver function tests, bleeding profile over different days among the studied patients:

	RDW first day		RDW fourth day		RDW seventh day	
	r	p	r	p	r	p
CRP (mg/l)	0.444	0.004*	0.358	0.023*	0.042	0.795
S. Creatinine (mg/dl)	-0.049	0.763	0.106	0.516	0.029	0.858
BUN (mg/dl)	0.042	0.795	0.102	0.531	0.045	0.781
ALT (U/l)	-0.044	0.786	-0.088	0.588	0.031	0.848
AST (U/l)	0.2	0.217	0.161	0.322	0.147	0.346
PT (Sec)	0.028	0.865	-0.005	0.974	-0.092	0.572
PTT. (Sec)	0.101	0.534	0.273	0.089	0.05	0.758
INR	0.065	0.69	0.163	0.316	0.084	0.605

CRP, C-reactive protein; BUN, blood urea nitrogen; ALT, **alanine** aminotransferase; AST, aspartate aminotransferase; PT, prothrombin time; PTT, partial thromboplastin time; INR, international normalized ratio

Table 6 Relation between RDW on different days and mechanical ventilation among the studied patients:

RDW %	Mechanical ventilation		Test	
	No (n=18)	Yes(n=22)	t	p
	Mean ± SD	Mean ± SD		
First day	16.72±3.63	15.92±3.31	0.727	0.472
Fourth day	16.87 ± 2.87	15.95±4.01	0.823	0.415
Seventh day	17.08 ± 3.6	16.22 ± 2.87	0.846	0.403
p (F)	0.868	0.877		

Table 7 Performance of RDW on first, fourth and seventh days respectively in prediction of mortality among the studied patients:

Cutoff	AUC	Sensitivity	Specificity	PPV	NPV	+LR	-LR	Accuracy	p
≥17.6	0.896	100	75.7	25	100	4.12	0	77.5	0.024*
≥18.05	0.622	66.7	78.4	20	96.7	3.09	0.42	77.5	0.488
≥15.55	0.532	62.2	100	100	88.5	0	0.38	57.5	0.857

*, P<0.05 is statistically significant; PPV, positive predictive value; NPV, negative predictive value; +LR, positive likelihood ratio; -LR, negative likelihood ratio

DISCUSSION

Several earlier studies have evaluated, defined, and used CT as the best technique in head and neck imaging and neck mass measurement and recorded a much higher resolution than other available methods [8]. MDCT is a non-invasive technique characterised by short scanning times, fast imaging, high spatial resolution, and a Z-axis orientation with a higher isotropic orientation. The robust post-treatment function allows MSCT to observe lesions from different angles, and one of its disadvantages is that it is relatively highly exposed to ionising radiation compared to an MRI [9]. The present research involved 18 patients, 61.1 percent of whom were women and 38.9 percent were males. Equal distribution between men and women was documented in both Vaughn [10] and Hudise et al. [11], which reported that out of 62 patients (33 men, 53.2% and 29 women, 46.8%), The age range of presentation was 1 to 14

years; the majority of cases developed in children aged 6 to 10 years and in children aged 11 to 14 years, both 38.7%, whereas Gupta et al. [12] reported that the age range in the study was 3 to 80 years. According to Hudise et al. [11], the largest group of patients (36%) was between the ages of 0 and 20, with the second largest group (31%), between the ages of 51 and 70. The research found that four cervical abscess patients showed standard radiological characteristics of central hypodensity with peripheral rim enhancement and were officially diagnosed using contrast-enhanced multi-detector CT conducted by Gupta et al. [12]. In this experiment, the CT features of facial and neck infection swellings showed 22 percent well-defined edges, 16 percent hypodensities, 11 percent peripheral wall enhancement, and 11 percent full enhancement. MDCT identified 31 (51.7%) patients with benign neck masses and 29 (48.3%) patients with malignant neck masses. It confirmed that MDCT had high sensitivity and accuracy in identifying

benign and malignant neck mass lesions, which allows for preparation of these lesions for further management but requires histopathology for better management. mentioned by Chandra et al. [13]

The current study indicates that the RT side of the face and thyroid nodules in the left thyroid lobe have a benign soft tissue tumour (lipoma). The lipoma was seen in CT with hypodense fat attenuation and no contrast enhancement, as previously described. This is in conformity with the findings reported by Gupta et al. [12], where they stated that the MDCT confirmed the diagnosis of lipoma in one patient on the basis of the characteristic fat attenuation of the lesion, in addition to clearly demonstrating the lesion extension and confirming it during surgery.

The current study found that bone tumors, one case of fibrous dysplasia in the RT face, and thalassemia destruction of the right mandibular ramus were all present. Fibrous dysplasia manifested as a well-defined solid cystic lesion with septation and turbid fluid on ultrasound and as a well-defined expansile osteolytic lesion with a thin sclerotic margin, no contrast enhancement, and no fluid-fluid level on CT. After a complete investigation and consultation with physicians, we divided patients into 3 groups according to their treatment decisions: Surgical in 7 cases thyroglossal cyst, branchial cleft cyst, lipoma, ranula, left thyroid nodule, submental abscess, and fibrous dysplasia Except for fibrous dysplasia, which was a false negative, all of the cases were confirmed by CT diagnosis and surgery. Surgery confirmed the CT diagnosis of an aneurysmal bone cyst, and histopathology revealed fibrous dysplasia.

Medical in 6 cases 2 cases of infantile hemangioma, one case of thalassemia, and one case of infected LN, periorbital cellulitis, and parotitis All the medical cases confirmed the CT diagnosis through treatment and follow-up. The two infantile hemangiomas were treated with propranolol for 6 months to a year with follow-up, and the thalassemia case was transferred to the haematology department for blood transfusion and treatment, while the other infected cases responded successfully to treatment.

And the final Sclerotherapy treatment in five cases: two of venous malformation, two of lymphatic malformation, and one of hemangioma.

In the present study, the MDCT diagnosis was confirmed in 33.3% of cases by medical treatment and follow-up, 33.3% by surgery and histopathology, and 22.2% by MRI in vascular anomalies of the face and neck.

The MDCT diagnosis was incorrect in two cases: one case of fibrous dysplasia, which was confirmed by surgery and histopathology, and one case of hemangioma, which was confirmed by MRI.

In this study, there were 7 cases of vascular swellings, with hemangioma (3 cases), venous malformation (2 cases), and lymphatic malformation (11.11% of them, 2 cases).

In the study performed by Gupta et al. [12], seven patients with vascular malformations, six patients with low vascular malformations, and one patient with high vascular malformations were evaluated. Two cases of lymphatic malformation showed well-defined peripheral by homogeneous contrast enhancement, while two cases of venous malformation showed ill-defined isodense attenuation of the same muscle with phleboliths. In four patients, lymphangiomas were correctly diagnosed on multislice CT; all the lesions were well defined with homogenous fluid attenuation, and the lesions in five patients with low-flow vascular malformations showed typical muscle attenuation with mild to moderate, heterogenous post-contrast enhancement with ill-defined margins. In agreement with the data study, this has shown that the bone tumors, one case of fibrous dysplasia located in the RT face, and thalassemia destruction of the right mandibular ramus

Fibrous dysplasia showed a well-defined hard cystic lesion with septation and turbid fluid in CT and a well-defined expansive osteolytic lesion with no contrast enhancement and no fluid-fluid level in CT with a thin sclerotic margin. After comprehensive investigation and consultation with doctors, patients were divided into three groups according to the treatment decision: thyroglossal cyst, branchial cleft cyst, lipoma, ranula, left thyroid nodule, sub-mental abscess, and fibrous dysplasia in 7 surgical instances.

All cases were confirmed by CT and surgery, with the exception of fibrous dysplasia, a false negative CT diagnosis that was diagnostic but not definitive. Medical in 6 cases 2 cases of infantile hemangioma, one case of thalassemia, and one case of infected LN, periorbital cellulitis, and parotitis The CT diagnosis has been confirmed by treatment and follow-up in all medical cases. Of the 2 cases of infantile hemangioma treated with propranolol after 6 months to 1 year of follow-up and the thalassemia case transferred to the blood transfusion and treatment department of hematology, other infected cases responded successfully to treatment. In 5 cases, the last sclerotherapy care was provided in 2 cases of venous malformation, 2 cases of lymphatic malformation, and 1 case of hemangioma. In the current study, the MDCT diagnosis was confirmed in 33.3 percent of cases by medical care and follow-up, 33.3% by surgery and histopathology, and 22.2 percent by MRI in cases of facial and neck swelling and vascular abnormalities.

The current study found that 60% of sclerotherapy cases had complete lesion obliteration, which were cases of lymphatic malformation with hemangioma, and 40% had partial lesion obliteration (2 cases of venous malformation).

Lee et al. [14] showed that the immediate success rate of the sclerotherapy in 98 sessions for 30 patients was 92% (90/98) with failure in 8% (8/98). Of the eight failed sessions, seven failed because of the lesion's inaccessibility, due to a lack of proper veins for direct puncture technique, to the nidus to deliver the scleroagent, and one failed session was the premature interruption of the therapy due to the fear of extension of the thrombus by the scleroagent from the malformed vein to the normal deep vein, which are directly connected to each other. Adams et al. [15] reported a high rate of excellent outcomes with sclerotherapy or surgical excision for macrocystic lymphatic malformations, with a 76% to 95% success rate.

The sensitivity of MDCT in this study was 87.5%, the specificity was 100%, the PPV was 100%, the NPV was 50%, and the accuracy was 90%.

Wang et al. [16] show that cross-sectional imaging is necessary for better localization of the lesions; the most promising technique is CT with contrast enhancement of the neck and thoracic, with a sensitivity of 64–100% and a specificity of 45–82%.

CONCLUSION

Multidetector Computed Tomography (MDCT) imaging is useful for quick and accurate assessment of facial and neck swelling, as well as the possibility of improving any vascular territory in facial and neck swellings using interventional radiology's minimally invasive technique.

Conflict of Interest: None.

Financial Disclosures: None.

Supplementary Files: Tables S1, S2, S3 and Figures S1 and S2.

REFERENCES

- 1- Brown R, Harave S. Diagnostic imaging of benign and malignant neck masses in children-a pictorial review. *Quant Imaging Med Surg* 2016; 6 (5): 591-604.
- 2- de Santana-Santos T, de Souza-Santos J, Martins-Filho P, da Silva LC, Silva E, Gomes A. Prediction of postoperative facial swelling, pain and trismus following third molar surgery based on preoperative variables. *Med Oral Patol Oral Cir Bucal* 2013; 18(1): e65.
- 3 -Robertson R, Silk S, Ecklund K, Bixby S, Voss S, Robson C. Imaging optimization in children. *J Am Coll Radiol*. 2018; 15(3):440-43.
- 4- Carlton J, Maxwell A, Bauer L, McElroy S, Layfield L, Ahsan H et al. Computed tomography detection

of extracapsular spread of squamous cell carcinoma of the head and neck in metastatic cervical lymph nodes. *Neuroradiol J* 2017; 30(3): 222-29.

- 5- Bagale S, Agarwal V, Dethe V. Multi Detector Computed Tomography Evaluation of Neck Masses in Adults. *Inter J Contem Med Surg Radiol* 2017; 2(4): 127-132.
- 6- Krüger R, Hilker R, Winkler C, Lorrain M, Hahne M, Redecker C et al. Advanced stages of PD: interventional therapies and related patient-centered care. *J Neural Transm* 2016; 123(1): 31-43.
- 7- Kulkarni S, Shetty N, Dharia T, Polnaya A. Pictorial essay: Vascular interventions in extra cranial head and neck. *Indian J Radiol Imaging* 2012; 22 (4): 350-57.
- 8- Badawy MK. Pediatric neck masses. *Clin Pediatr Emerg Med* 2010; 11 (2) : 73-80.
- 9- Irani S, Bidari Z, Sabeti S. Prevalence of pathological entities in neck masses: A study of 1208 consecutive cases. *Avicenna J Dent Res* 2016; 8 (1): e25614.
- 10- Vaughn J Imaging of pediatric congenital cystic neck masses. *Operative Techniques in Otolaryngology. Head Neck Surg* 2017; 28 (3): 143-50.
- 11- Hudise J. Y. Alshehri K. A. Shamakhey R. E et al. Prevalence and pattern of neck masses in pediatric patient: in Aseer Central Hospital, KSA. *Inter J Otorhinol Head Neck Surg* 2017; 3(4): 791-94.
- 12- Gupta P. Bhargava S, Mehrotra G, Rathi V. Role of multislice spiral CT in the evaluation of neck masses. *J Inter Med Sci Acad* 2013; 26 (1): 51-4.
- 13- Chandra D, Netam S, Sanjeev K, Renuka G, Varsha M, Anand J. Role of Multidetector Computed Tomography Scan in Evaluation of Neck Mass. *Inter J Sci Study* 2018; Vol 5 (11): 80-5.
- 14- Lee B, Kim D, Huh S, Kim H, Choo I, Byun H et al. Do YS. New experiences with absolute ethanol sclerotherapy in the management of a complex form of congenital venous malformation. *J Vasc Surg*. 2001; 33 (4) : 764-72.
- 15- Adams M, Saltzman B, Perkins J. Head and neck lymphatic malformation treatment: a systematic review. *Otolaryngol Head Neck Surg* 2013; 147(4):627–39.
- 16- Wang B, Gao B, Xu G, Xiang C. Images of deep neck space infection and the clinical significance. *Acta Radiol*. 2014; 55 (8) : 945-51.

To Cite:

Hassan, D, Khamis, M., Bessar, A Alsenosi, E., Multi Detector Computed Tomography Application in Diagnosis and Interventional Management of Facial and Neck Swellings in Children. *Zagazig University Medical Journal*, 2023; (485-495): -.doi: 10.21608/zumj.2021.54107.2055.

SUPPLEMENTARY FILES

Table S1 Percent of final diagnosis by CT (N=18):

MDCT	medical TTT			Surgical			Sclerotherapy		
	+ve %	_ve %	Total	+ve %	_ve %	Total	+ve %	_ve %	Total
+ve	6 33.3%	0 0%	6 33.3%	6 33.3%	0 0%	6 33.3%	4 22.2%	0 0%	4 22.2%
_ve	0 0%	12 66.6%	12 66.6%	1 5.55%	11 61.1%	12 66.6%	1 5.5%	13 72.2%	14 77.7%
Total	6 33.3%	12 66.6%	18 100%	7 38.8%	11 61.1%	18 100%	5 27.7%	13 72.2%	18 100%

Table S2 Validity of MDCT in detecting facial and neck swellings:

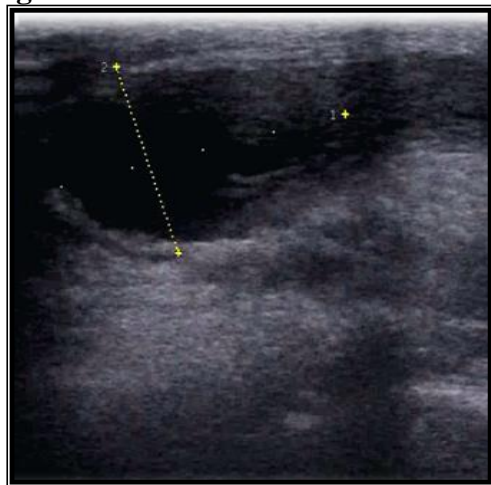
SN (%)	87.5%
SP (%)	100%
PPV (%)	100%
NPV (%)	50.0%
Acc (%)	90.0%

SN: Sensitivity, SP: Specificity, PPV: Positive Predictive Value, NPV: Negative Predictive Value, Acc: Accuracy.

Table S3 Results of sclerotherapy among intervention group:

Variable	No.=5	%
Sclerotherapy:		
Complete lesion obliteration	3	60
Partial lesion obliteration	2	40

Figures:



(A)



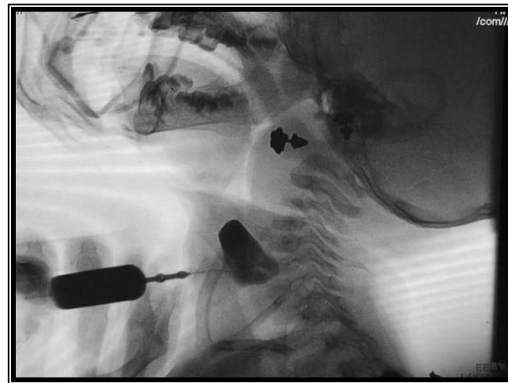
(B)



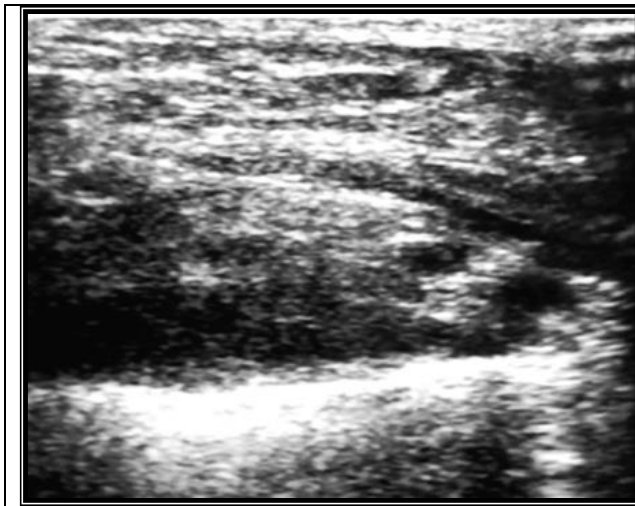
(C T1)



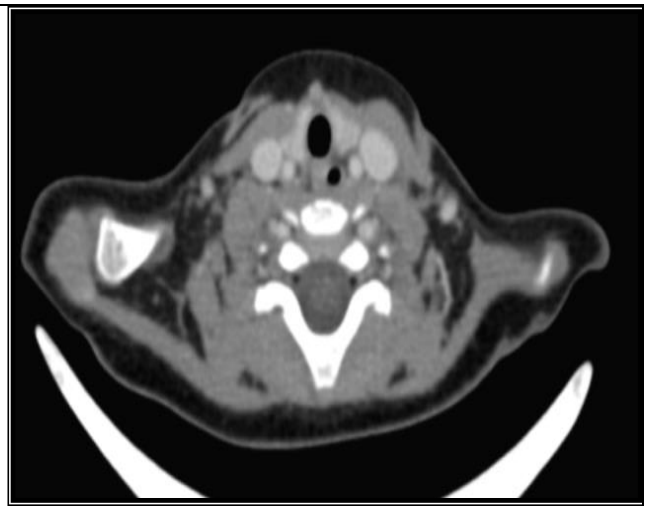
(C T2)



(D)

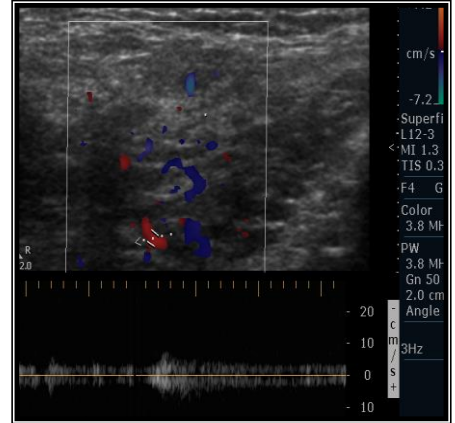
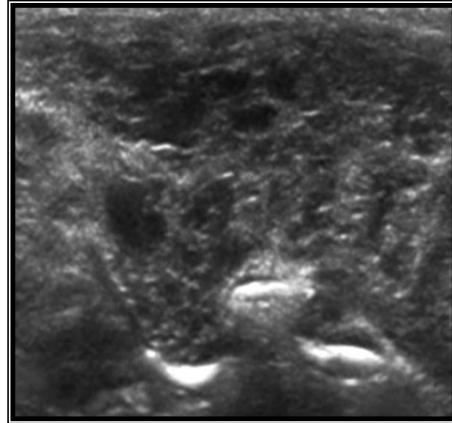


(E)



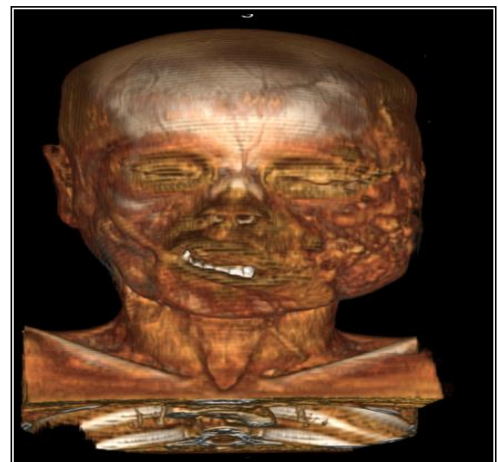
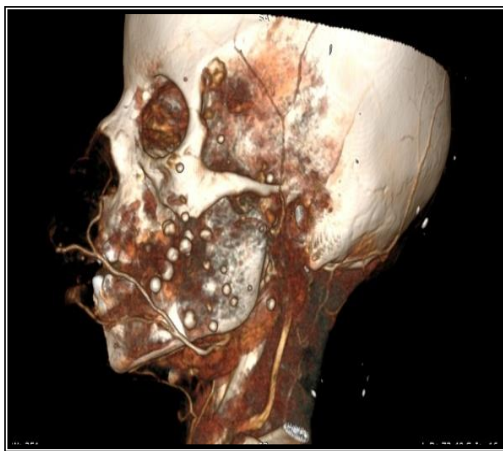
(F)

Fig. S1 A case of macrocytic lymphatic malformation (A) *Ultrasound*: shows well circumscribed cystic lesion in supra clavicular region measuring about 2x6cm, no calcification or color flow, (B) *CT with contrast*: appear cystic lesion in left posterior triangle with no extension to the thoracic inlet, (C) *MRI*: coronal MR T1 & T2 show isointense cystic lesion in left posterior triangle, (D) *Sclerotherapy*: Interventional procedure fluoroscopic image for percutaneous needle injection bleomycin in lymphatic malformation in LT posterior triangle of the neck under general anesthesia. (E) *Ultrasound after sclerotherapy*: show complete obliteration of lymphatic malformation in left posterior triangle, supraclavicular region in ultrasound, (F): *Axial CT with contrast*: after complete sclerotherapy treatment and complete obliteration.

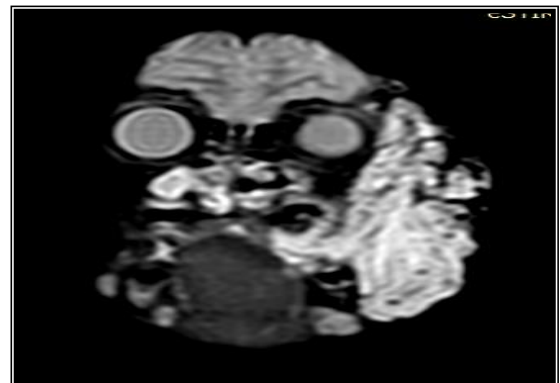


(A)

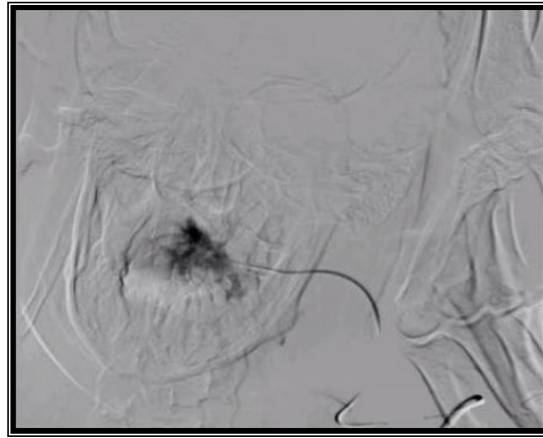
(B)



(C)



(D)



(E)

Fig. S2 Female patient with venous malformation, 10 years old complain left facial swelling since at birth, rubbery and pulsatile by physical examination. (A) *US examination*: homogenous small poly cystic (lacunar) lesion in subcutaneous and inter muscular separated by thin wall. (B) *Doppler Study*: shows monophasic waveforms with low blood flow). (C) *3D*: reformate shows VM phleboliths. (D) *MRI*: Coronal T1WI & sagittal T2WI show low signal foci within the ill -defined lesion representing phleboliths in the left face. (E) *Sclerothearpy*: Fluoroscopic image for percutaneous needle injection ethanol in venous malformation in LT face and upper lip under general anesthesia. (F) *MRI after sclerothearpy by 6 months*: Coronal TIWI with contrast & sagittal TIWI show well defined lesion isointense with skeletal muscle with few phlebolits high signal.



(F)